

# Clustering of Approaches to Microbiological Image Enhancement and Classification Based on Buser & Baroni-Urbani's Algorithm and Dragomirescu's Homogeneity

Alexandru-Ionuț Petrișor\*, Liviu Dragomirescu\*\*  
Alan W. Decho\*\*\*

\*Department of Urban and Spatial Planning, "Ion Mincu" University of Architecture and Urbanism, Bucharest 010014, Romania (Tel: 4-021-307-7133; e-mail: alexandru\_petrisor@yahoo.com).

\*\*Department of Ecology, Faculty of Biology, University of Bucharest, Bucharest 050095, Romania (e-mail: liviu\_dragomirescu@yahoo.com)

\*\*\* Department of Environmental Health Sciences, Norman J. Arnold School of Public Health, University of South Carolina, Columbia, SC 29208, USA (e-mail: [awdecho@mailbox.sc.edu](mailto:awdecho@mailbox.sc.edu))

**Abstract:** Even though microbial imagery had constantly benefited upon technical developments, the analysis of microbial images did not record the same progress. However, analytical tools had been developed in conjunction with remote sensing imagery, and are available for other fields of study as well. When importing such approaches, it is necessary to understand their detailed functioning in order to envisage eventual problems and improve the correctness and accuracy of results. The paper analyzes several approaches to microbial imagery enhancement, quantification, and classification. Approaches are classified using a numerical taxonomy instrument, i.e. Buser & Baroni-Urbani's algorithm and Dragomirescu's homogeneity. Results indicate the presence of three methodological groups and sustain the usage of the image classification/GIS methods in microbiology and other biological fields.

**Keywords:** remote sensing; image classification; numerical taxonomy; homogeneity; confocal microscopy.

## 1. INTRODUCTION

Bacterial cells, upon attachment to surfaces, envelope themselves within a matrix of secreted extra-cellular polymeric substances to form biofilms under a range of environmental conditions (Kuehn *et al.*, 1998). Biofilms have important economic, medical, and environmental roles (Stoodley *et al.*, 2002). The study of the in-situ properties of biofilms has been facilitated by advances in microscopy, such as the confocal scanning laser microscopy (CSLM) used in conjunction with analytical imaging (Korber *et al.*, 1993), digital analysis (Lewandowski *et al.*, 1999), and semi-automated image processing (Kuehn *et al.*, 1998). Various approaches have been developed based on CSLM in order to assess the structure (Kuehn *et al.*, 1998) and spatial variability within biofilms (Korber *et al.*, 1993). Stromatolites are the oldest known fossil macrostructures, dating back more than 3.5 billion years, still forming in isolated areas of the Bahamas (Reid *et al.*, 2000) through bacterial processes including biofilm formation.

Bacterial and biofilm images can be acquired using different microscopy techniques, such as analogue techniques (dark-field microscopy, phase-contrast microscopy, interference microscopy, or fluorescence microscopy), and analytical (CSLM) - Lewandowski *et al.*, 1999. Images are processed using various enhancement techniques, such as mathematical filtration, de-convolution, intensity correction, thresholding,

cleaning, difference imagery, pseudo-colour, contrast stretching (Lawrence *et al.*, 1997), and finally classified. The classification process may extract specific elements (feature extraction), or assign each individual pixel to a category (complete classification). There are two types of image classification (Jensen, 1996). Supervised classification allows trained users to select sample pixels corresponding to each feature within the image to define specific signatures, and later the computer performs the classification based on the collection of signatures. Unsupervised classification is performed by the computer based on threshold values or final number of classes. "Feature Analyst", presented in this paper, has been used only for unsupervised image classification.

The outcomes are enumeration of bacteria, determination of growth, viability, and metabolic conditions, assessment of the microstructure of biofilm, micro-environmental analyses, quantification of biodiversity, and computer control of microscope stage (Lawrence *et al.*, 1997).

Different techniques currently used in geography, geology, environmental sciences (University of South Carolina, 2003), and other fields to study small-scale phenomena have recently found applications at larger scales (Chon and Schneider, 2001). However, studies at smaller spatial scales, are similar in principle to quantifying sizes of bacterial cells using confocal microscopy. A second application of remote sensing at an individual level used a "close sensor" to measure "shapes" of various body surfaces in human

subjects, such as faces, backs, and torsos for medical purposes, as well as dynamics of the human body (Mitchell, 1995). Similar methodologies may be developed for biofilms and bacteria using appropriate sensors.

Moreover, medical imagery has been used for a long time. A quick screening of the latest developments in the field reveals the presence of approaches designed to reconstitute the three-dimensional structure of the biliary tree (Chen and Wang, 2004a) or spinal nerves (Chen and Wang, 2004b) from magnetic resonance images. Different image processing techniques were employed to differentiate malignant metastatic tumour infiltration from benign fracture oedema based on colour intensity (Park *et al.*, 2004), detect bladder tumours (Yazgan *et al.*, 2004), identify reductions in the grey matter density concentrated in the frontal and cingulate gyri, particularly in the right hemisphere of bipolar patients (Doris *et al.*, 2004), find tumours and assess their reaction to different treatments (Kluetz *et al.*, 2000), evaluate the extent of Erdheim-Chester disease and the response to therapy (Neto *et al.*, 2004). Classification and registration of magnetic resonance images were used in conjunction with statistical analyses to study cerebral atrophy in late-onset dementia (Paling *et al.*, 2004), and psychological dispositions, *i.e.*, sadness vs. happiness (Killgore and Yurgelun-Todd, 2004). Image analysis techniques, such as convolution, were used in conjunction with numerical techniques to track neuronal fibers in magnetic resonance images (McGraw, 2004). In summary, the medical imagery offers a wide range of techniques, including quantitative methods.

Confocal microscopy, by design, is a type of remote sensing, since it involves "the acquiring of data about an object without touching it" (Jensen, 2000). Simplistically, and ignoring the special path of light in aerial photography or confocal microscopy, it may be argued that the major difference between remote sensing of biofilms using confocal microscopy and remote sensing of the Earth using aerial photography or satellite imagery is simply one of "scale" (Petrişor *et al.*, 2003), as displayed in Figure 1a.

Cowen (1988) has argued that the main purpose of remote sensing, particularly aerial photography, has been to provide data for the Geographic Information Systems (GIS). A GIS may be defined as a "decision support system involving the integration of spatially referenced data in a problem solving environment" (Cowen, 1988). Traditionally, GIS has been used at small-scale. Applications in microbiology have concerned mapping the concentration of indicator species of microorganisms, such as faecal coliforms, based on sampling stations distributed along some transects (Kistemann *et al.*, 2001) or monitoring microbial degradation of toxic compounds in coastal areas (Fedra and Feoli, 1998). From a methodological perspective, this research represents an extension of the traditional use of GIS to spatial analysis of biofilm maps, and change detection within biofilms due to different environmental conditions (Figure 1b).

In analyses of satellite images a ground truth can always be determined, microbiological experiments used fluorescent microspheres of known sizes as a ground truth.

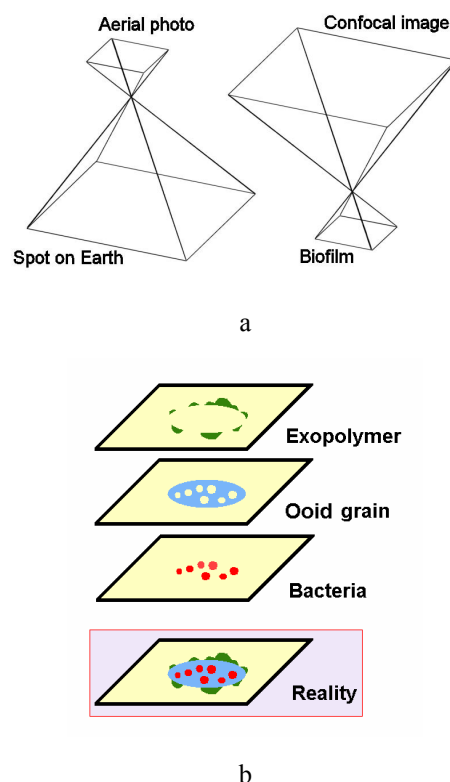


Fig. 1. If the details related to the path of light in aerial photography and confocal microscopy are ignored, the difference between the two examples of remote sensing reduces to scale (a). Results can in both cases analyzed using GIS techniques. In the microbiological realm, interpretations are provided from the viewpoint of a "bacterial GIS" (b)

The procedures used in geographic analyses had been in place for a long time. Therefore, the intrinsic detailed operation of these tools has been designed along with their operation. For example, a high-pass filter has always been used to enhance edges of features within images (Jensen, 1996). However, the application of these methods in the field of microbiology may result in the development of specific tools that can be eventually used in the analysis and classification of bacterial images.

This paper aims to use numerical taxonomy tools to reveal eventual clusters formed by different digital image processing and classification methods used in microbial ecology.

## 2. MATERIALS AND METHODS

Three sets of images were used. The first two sets of images displayed an artificial system, *i.e.* polymeric microspheres, either alone (set #1,  $N=30$ ) or embedded in gel capsules (set #2,  $N=9$ ), whilst the third one (set #3,  $N=10$ ) consisted of images of microscopical sections through stromatolites.

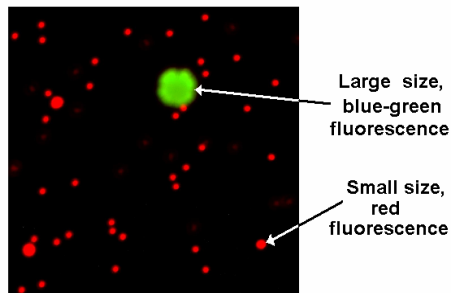
Set #1 consists of sections through the equator of fluorescent microspheres (Figure 2a). Only the equatorial sections were used in this experiment, under the assumption of the manufacturer that the diameter of such microspheres is 1  $\mu\text{m}$ .

Consequently,

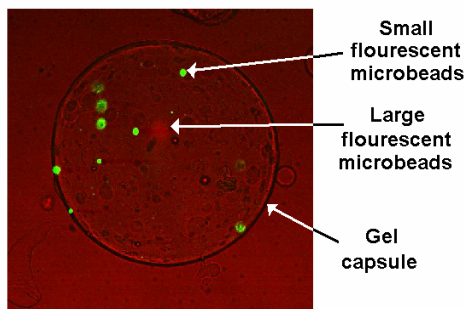
$$A = \pi r^2 = \pi \left(\frac{d}{2}\right)^2 = \frac{\pi d^2}{4} = \frac{3.1415}{4} = 0.7854 \mu m^2 \quad (1)$$

As the size of each pixel was  $1/144.26 \mu m$  (microscopical stage control), the area in pixels is:

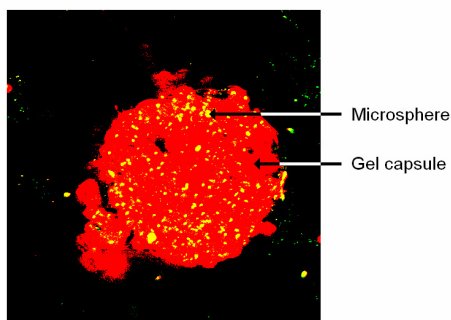
$$A = 0.7854 / \left(\frac{1}{144.26}\right)^2 = 16344.92 \text{ square pixels}$$



a



b



c

Fig. 2. Fluorescent microspheres used for the calibration of the GIS-based approach individually (a) or embedded into gel capsules, fluorescent (c) or not (b)

Set #2 increase the degree of complexity of the "ground reality" by embedding microspheres into gel capsules (Moslemy *et al.*, 2002) in order to simulate the natural

biofilm of marine stromatolite environments (Figure 2 b and c). The fluorescence of microspheres and gel capsules overlapped, therefore the assumption of a known and constant diameter of microspheres does not hold in this case.

Set #3 attained the maximum complexity and consisted of images of sections through marine stromatolites.

The final output of the microscopic stage was represented by black and white or colour images saved in a specific format (PIC), viewed with an application called "Confocal Assistant" (Brelje, 2003), or by coloured composite images exported in a Bitmap format. Following acquisition, image files were eventually converted to a Joint Photographic Experts Group (JPEG) format or a JPEG-compatible format, or Tagged Image File Format (TIFF).

The main methods were: (1) Unsupervised classification using Feature Analyst: this new tool, developed as an extension of ArcView GIS and ArcGIS, incorporates all the following techniques of image enhancement, performing also the unsupervised classification of images. The classification process is based on the final number of classes, defined by the user (Feature Analyst, (2003); (2) Contrast stretching by histogram equalization (in order to eliminate the noise and facilitate the separation of bacteria from the background), followed by unsupervised classification using Erdas Imagine 8.5 (Jensen, 1996 and 2000; ERDAS, 2003); (3) Filtration using a 3 x 3 high-pass filter, followed by unsupervised classification using Erdas Imagine 8.5 (Jensen, 2000; ERDAS, 2003); (4) Combinations of methods 2) and 3) in different order (the unsupervised classification was performed only once, in the final, following contrast stretching and filtration); (5) Unsupervised classification of raw images using Erdas Imagine 8.5, based also on the final number of classes, defined by the user (ERDAS, 2003); (6) For images from sets #2 and #3, supervised classification using Erdas Imagine 8.5 based on selection of representative pixels for each category by the user, followed by the classification of the entire image by the computer based on the classes defined by sampled pixels (ERDAS, 2003).

To illustrate the steps presented above, Figure 3 presents several procedures using as an example images of a section through a biofilm.

The analysis attempted to answer several questions. The first one refers to the quantification of the differences between the methods, and also to their accuracy and precision. However, it is more interesting to analyze the intrinsic mechanism of these methods. The discussion pertains to the pixel level; based on the choice of one classification algorithm, and on the enhancement of images, each pixel is assigned to some class. The question is whether an algorithm tends to preferentially assign pixels that in reality correspond to some class to another one, and the statistical instruments to answer such questions, if existing, are not easily available. If pixels in set #1 belong to the "microsphere" or to the "background", set #2 contains pixels belonging to the "microspheres", "gel capsules or parts of these", and "background". The composition of images from set #3 is even more complex;

microbiologists might distinguish between "oid grains", "endolithic bacteria", "cyanobacteria", "exopolymer", and "microbored canals". However, not all these features appear in each image, therefore a simpler classification distinguishes between "oid grains", "exopolymer", and "canals". Differences are expected between supervised classification, where the trained user is looking for specific features, and unsupervised classification, based in all these examples on the generation of a fixed number of classes, despite their composition or correspondence to the theoretical classes used in supervised classification. Consequently, statistical analyses used to compare the image processing approaches varied from one set to another.

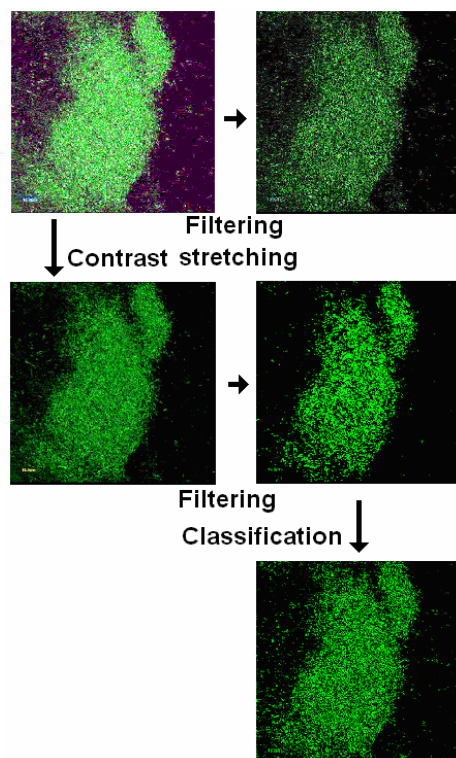


Fig. 3. Illustration of several image enhancement and classification techniques, using a section through a biofilm.

Set #1: the methods used to enhance and classify images of the equatorial sections through fluorescent microspheres were compared using SAS (Cody and Smith, 1997). The mean area for each method was statistically compared with the theoretical mean (16344.92 squared pixels) using t-tests. The analysis of variance has been used to analyze whether there are significant differences between the methods. To analyze the origin of the differences, several post-hoc approaches were used: Duncan Multiple Range test, Waller-Duncan K-ratio t test, Tukey Studentized Range test, Studentized Maximum Modulus (GT2) test, Bonferroni (Dunn) t test, and Scheffé's test (Cody and Smith, 1997).

Sets #2 and #3: statistical analyses attempt to answer the question whether there are significant differences between the methods, but not whether some of them preferentially diminish or dilate some class. A classification of approaches has been performed using Buser & Baroni-Urbani's classification method (Buser and Baroni-Urbani, 1982),

modified in two steps, to yield a single result almost every time (Dragomirescu, 1987 and 2003; Dragomirescu and Postelnicu, 2003). The analyses were performed using a Basic application (Dragomirescu, 2003). The methods used for the classification and enhancement of images of equatorial sections through the fluorescent microspheres could not be classified with this method.

The classification method is an algorithm proposed by Buser and Baroni-Urbani (1982), modified by Dragomirescu (1987). Previous uses of the methodology include the classification of land parcels based upon vegetation coverage (Biță and Dragomirescu, 2006) or thickness of the peat layer (Timofti, 2004).

### 3. RESULTS

For Set #1, the F-test was 42.23, indicating very highly significant ( $p < 0.0001$ ) differences between the methods. All post-hoc approaches yielded the same result, finding three groups of approaches: (1) Contrast stretching used alone, and followed by filtration; (2) Filtration followed by contrast stretching; (3) Unsupervised classification of raw images in Erdas 8.5, unsupervised classification of filtered images in Erdas 8.5, and unsupervised classification of raw images using Feature Analyst.

A graphical illustration of the performance of the approaches is displayed in Figure 4. Table 1 presents the results of t-tests comparing the mean diameter of microspheres with the theoretical value.

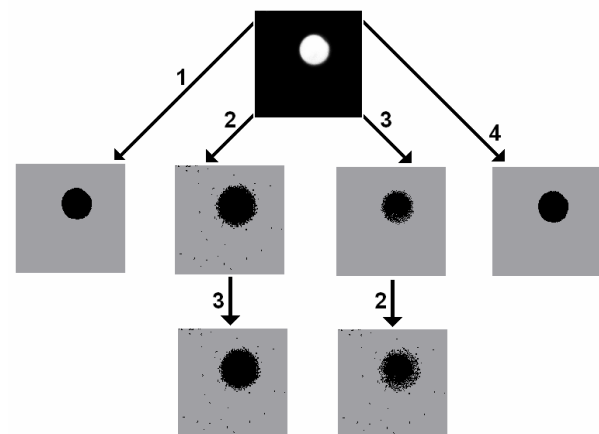
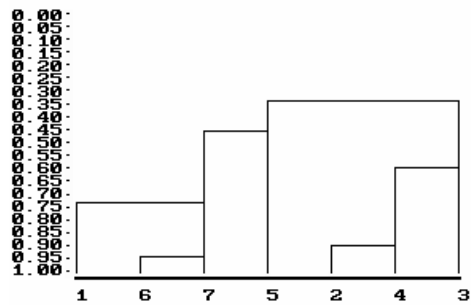


Fig. 4. Image enhancement and classification techniques illustrated using a representative image of a section through the equator of a fluorescent microsphere: 1- unsupervised classification using Feature Analyst (includes enhancement); 2- contrast stretching; 3- filtration; 4- unsupervised classification in Erdas Image 8.5.

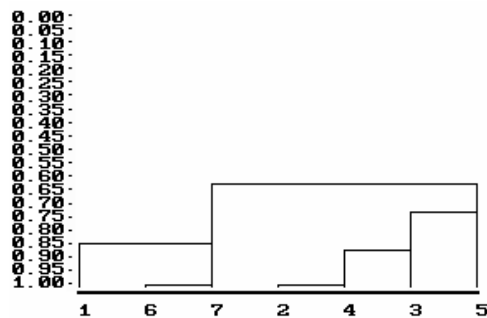
Figures 5 and 6 present the results obtained for the images from Set #2, while Figures 7 and 8 classify approaches used for images from Set #3. In both cases, the approaches were numbered as follows: (1) Unsupervised classification of raw images using Erdas Image 8.5; (2) Unsupervised classification of images following contrast stretching using Erdas Image 8.5; (3) Unsupervised classification of images



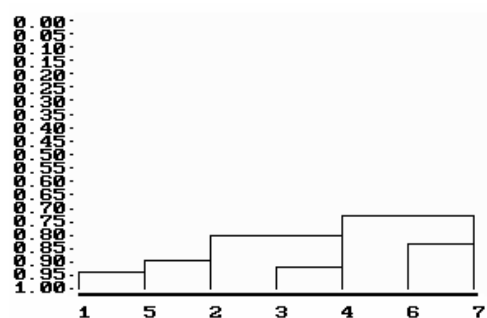
following filtration using Erdas Imagine 8.5; (4) Unsupervised classification of images following contrast stretching and filtration using Erdas Imagine 8.5; (5) Unsupervised classification of images following filtration and contrast stretching using Erdas Imagine 8.5; (6) Unsupervised classification of raw images using Feature Analyst; (7) Supervised classification of raw images using Erdas Imagine 8.5.



H homogeneity for multi-state tables



M1 homogeneity



M2 homogeneity

Fig. 5. Results of different classification schemes comparing the approaches used for the enhancement and classification of images of gel capsules embedding fluorescent microspheres.

#### 4. DISCUSSION

A visual overall analysis of images might reveal some details. The images exhibit significant visual differences with respect to the application of the methods described above. The simplest images indicate a dilation or contraction of the main feature (the section through the microsphere); more complex images exhibit the reduction of pixels belonging to one class

(microspheres embedded in the gel capsule, when contrast stretching is applied to either raw images or filtered images) or two classes (both embedded microspheres and gel capsules, when filtration is applied to the raw images). Finally, the most complex images exhibit such a great diversity, that their behaviour with respect to the techniques does not follow a predictable pattern.

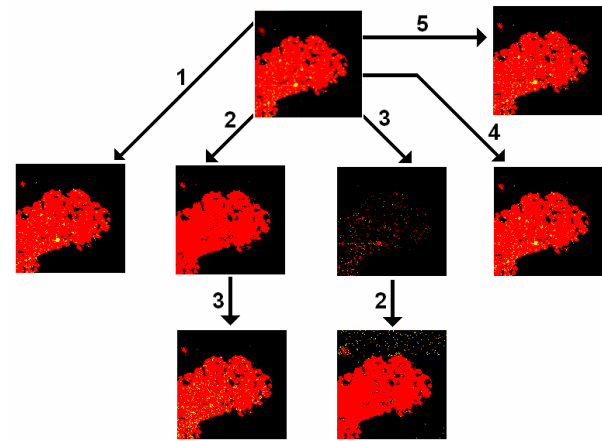


Fig. 6. Image enhancement and classification techniques illustrated using a representative image of a section through a gel capsule embedding fluorescent microspheres: 1- unsupervised classification using Feature Analyst (includes enhancement); 2- contrast stretching; 3- filtration; 4- unsupervised classification in Erdas Imagine 8.5; 5- supervised classification in Erdas Imagine 8.5.

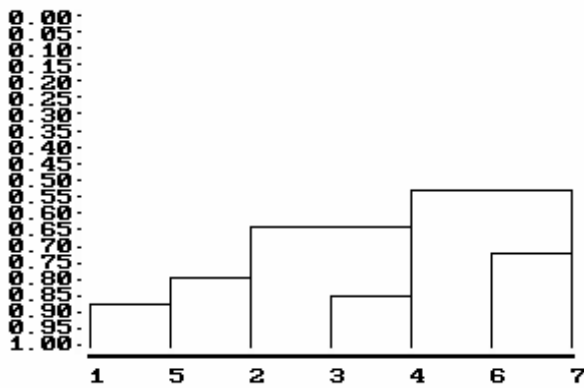
**Table 1.** Comparison of the enhancement and classification techniques used for images of equatorial sections of fluorescent microspheres: (1) Unsupervised classification of raw images using Erdas Imagine 8.5; (2) Unsupervised classification of images following contrast stretching using Erdas Imagine 8.5; (3) Unsupervised classification of images following filtration using Erdas Imagine 8.5; (4) Unsupervised classification of images following contrast stretching and filtration using Erdas Imagine 8.5; (5) Unsupervised classification of images following filtration and contrast stretching using Erdas Imagine 8.5; (6) Unsupervised classification of raw images using Feature Analyst

Method	Mean area occupied by the equatorial section	Standard deviation	T-test	p-value
1	16450	1992.8	0.29	0.7747
2	32390	10486	8.38	<0.0001
3	13383	2845.2	-5.70	<0.0001
4	31672	9960.5	8.43	<0.0001
5	25386	8413.8	5.89	<0.0001
6	16430	1887.7	0.25	0.8066

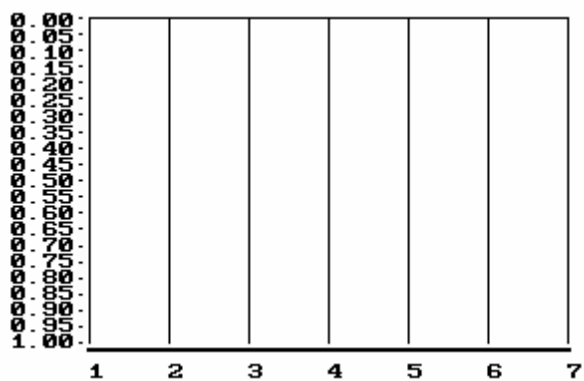
Supervised classification is, in fact, conceptually and pragmatically, the best approach to be used for complex images (Jensen, 1996). Therefore, the results are more accurate as the complexity of images increases. Unsupervised classification is, again conceptually and pragmatically, the best approach to be used for simpler images (Jensen, 1996), thus its accuracy decreases with the increase of complexity.

Feature Analyst seems to provide very accurate results, especially for lesser complex images, as it uses both supervised classification, the appropriate tool in this case, and a certain portion of the image enhancement techniques.

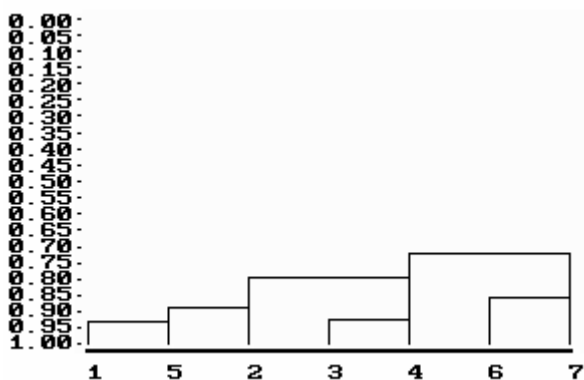
The reliability of the image classification process, which provided the data used in all spatial analyses described in this research, depends on the quality of images (Figure 9). The quality of the image is the result of the microscopic stage, i.e. of the combination of gain, opening of the iris, power of lasers, specificity of the lasers, and resolution. Resolution is particularly important; greyscale images are collections of pixels of different intensities (Figure 10).



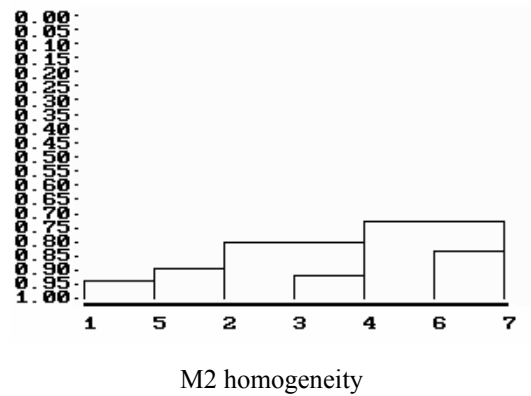
H homogeneity for multi-state tables



$p(\chi^2)$ , the probability of  $\chi^2$  in a contingency table



M1 homogeneity



M2 homogeneity

Fig. 7. Results of different classification schemes comparing the approaches used for the enhancement and classification of images of gel capsules embedding fluorescent microspheres

Colour images exhibit the same variability for each colour in a red-green-blue (RGB) format, i.e. they represent combinations of pixels of different intensities on a red, green, and blue scale. As the result, the identification of pixels specific to certain features becomes problematic in the edge regions, and produces different classification results. The size of such regions depends on the image resolution. Overall, the specificity of classification is a function of the resolution of images.

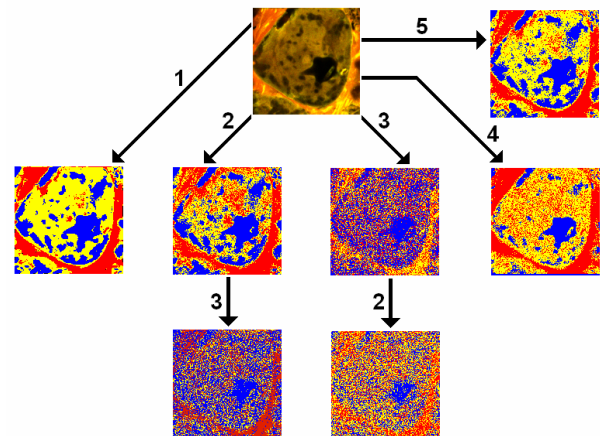


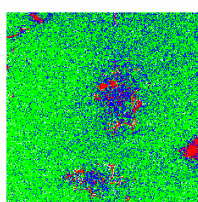
Fig. 8. Image enhancement and classification techniques illustrated using a representative image of a section through a stromatolite: 1- unsupervised classification using Feature Analyst (includes enhancement); 2- contrast stretching; 3- filtration; 4- supervised classification in Erdas Imagine 8.5; 5- unsupervised classification in Erdas Imagine 8.5.

For set #1, the results strengthen the analysis based on the visualization of images: estimations based on unsupervised classification of raw images do not differ statistically from the theoretical value when using Erdas Imagine 8.5 or the "Feature Analyst" extension of ArcView GIS. Filtration significantly decreases the estimate, whereas contrast stretching through histogram equalization increases the value significantly, when used alone, or in conjunction with filtration, either proceeding or following the latter. For sets #2 and #3, the interpretation of results is even more problematic than the statistical analysis.

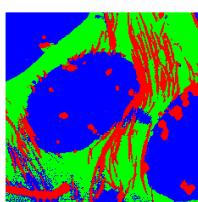
## 6. CONCLUSIONS

Therefore, considering the reduced size of the image data sets (particularly sets #2 and #3), the following statements must be interpreted as simple remarks rather than conclusions: (1) There is no clear clustering of the described classification methods; they vary conceptually and even more so when applied to sets of images of different complexities; (2) There is a similarity in the classification performed using unsupervised classification Feature Analyst or Erdas Imagine, and supervised classification (in Erdas Imagine); (3) The results regarding the classification of more complex images are not consistent with the ones obtained for simpler images, and also more difficult to interpret and explain; (4) For both sets, the following three groups contain similar methods: (a) Unsupervised classification of raw images using Erdas Imagine 8.5, unsupervised classification of images following contrast stretching using Erdas Imagine 8.5, and unsupervised classification of images following contrast stretching and filtration using Erdas Imagine 8.5; (b) Unsupervised classification of images following filtration using Erdas Imagine 8.5, and unsupervised classification of images following contrast stretching and filtration using Erdas Imagine 8.5; (c) Unsupervised classification of raw images using Feature Analyst, and supervised classification of raw images using Erdas Imagine 8.5.

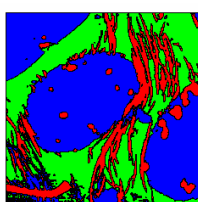
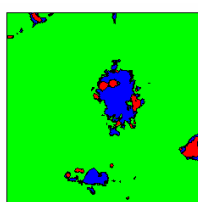
"Poor quality" image



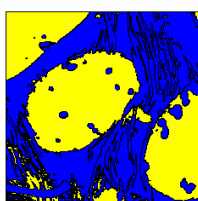
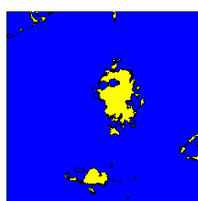
"Good quality" image



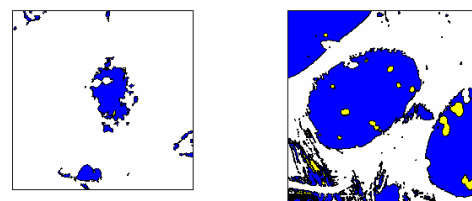
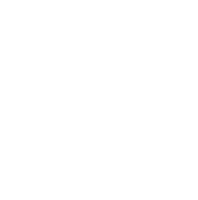
Supervised classification using three classes: EPS (green), ooid grains (blue), and microbored canals (red)



10 x 10 filter used to produce "smooth" images



Reclassification in two classes: ooid grains (yellow) and all other elements (blue)



Selection of the microbored canals (yellow) inside ooids (blue). Note that almost all canals in the first image are lost.

Fig. 9. Example of the effect of the quality of images on the final result

Overall, despite of inherent limitations, the methodology illustrated in this research represents a valuable asset. The powerful analytical tools of GIS were the only ones that could answer to research questions related to the spatial relationship between specific features: quantisation of microboring processes (Petrişor and Decho, 2004), calcification (Petrişor *et al.*, 2004 b) and orientation of cyanobacteria (Petrişor and Decho, 2006) in marine stromatolites, estimation of biovolumes (Petrişor *et al.*, 2004 a) or concentrations of homogeneous size particles (Petrişor and Decho, 2007). Results sustain the usage of the method in any biological field where potential applications can be foreseen.

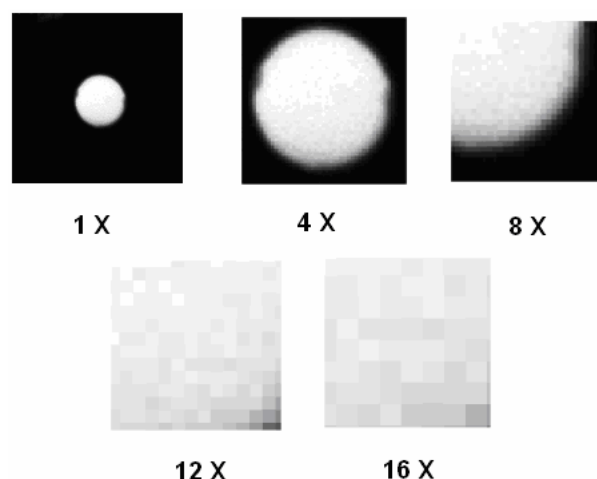


Fig. 10. Sections are not continuous, but collections of pixels of different intensity of light.

## ACKNOWLEDGEMENT

The authors would like to kindly thank Professor Ioan Dumitrache for his valuable comments that helped improving the quality of the manuscript.

## REFERENCES

- Biță, C., and Dragomirescu, L. (2006). Automated Classification Method Compatible with Zurich-Montpellier Phytosociological Method. 9th Conference of the Romanian Society of Statistics and Probabilities, Bucharest.

- Brelje, T.C. (2003). Confocal Assistant 4.02. Software for 3D analysis of confocal images, retrieved 11/24/2003 from <http://www.cyto.purdue.edu/flowcyt/software/cas402.htm>.
- Buser, M., and Baroni-Urbani, C. (1982). A direct non-dimensional clustering method for binary data. *Biometrics* 38, 360.
- Chen, Y.-T., and Wang, M.-S. (2004a). MR cholangiography 3D biliary tree automatic reconstruction system. *Computerized Medical Imaging and Graphics* 28, 13-20.
- Chen Y.-T., and Wang, M.-S. (2004b). Three-dimensional reconstruction and fusion for multi-modality spinal images. *Computerized Medical Imaging and Graphics* 28, 21-31.
- Chong, A.K., and Schneider, K. (2001). Two-Medium Photogrammetry for Bottlenose Dolphin Studies. *Photogrammetry Engineering and Remote Sensing* 67(5), 621-628.
- Cody, R.P., and Smith, J.K. (1997). *Applied Statistics and the SAS® Programming Language*, 138-141. Prentice Hall, Upper Saddle River, New Jersey.
- Cowen, D. J. (1988). GIS versus CAD versus DBMS: What Are the Differences? *Photogrammetric Engineering and Remote Sensing* 54, 1551-1555.
- Doris, A., Belton, E., Ebmeier, K.P., Glabus, M.F., and Marshall, I. (2004). Reduction of cingulate gray matter density in poor outcome bipolar illness. *Psychiatry Research: Neuroimaging* 130, 153-159.
- Dragomirescu, L. (1987). Some Extensions of Buser and Baroni-Urbani's Clustering Method. *Biometrical Journal* 29(3), 345-353.
- Dragomirescu, L. (2003). Clustering program by methods dedicated to biomedical thinking, *Proceedings of the 1st MEDINF International Conference on Medical Informatics and Engineering* 5(3) 146-147. Craiova, Romania.
- Dragomirescu, L., and Postelnicu, T. (1994). Specific numerical taxonomy methods in biological classification. In: Di Bacco, M., Pacciani E., and Borgognini Tarli S.M. (Ed.), *Statistical tools in human biology. Proceedings of the 17th Course of International School of Mathematics "G. Stampacchia"*, 31-45. World Scientific, London.
- ERDAS (2003). ERDAS Imagine Support, retrieved 11/24/2003 from <http://support.erdas.com>.
- Feature Analyst (2003). Feature Analyst, retrieved 11/25/2003 from <http://www.featureanalyst.com/index.html/support/support/Support.html>.
- Fedra, K., and Feoli, E. (1998). GIS Technology and Spatial Analysis in Coastal Zone Management. *EEZ Technology* 3, 171-179.
- Jensen, J.R. (1996). *Introductory Digital Image Processing. A Remote Sensing Perspective*, Prentice Hall, Upper Saddle River, New Jersey.
- Jensen, J.R. (2000). *Remote Sensing of the Environment. An Earth Resource Perspective*, Prentice Hall, Upper Saddle River, New Jersey.
- Killgore, W.D.S., and Yurgelun-Todd, D.A. (2004). Activation of the amygdala and anterior cingulate during nonconscious processing of sad versus happy faces. *NeuroImage* 21, 1215-1223.
- Kistemann, T., Dangendorf, F., and Exner, M. (2001). A Geographical Information System (GIS) as a Tool for Microbial Risk Assessment in Catchment Areas of Drinking Water Reservoirs. *International Journal of Hygiene and Environmental Health* 203, 225-233.
- Kluetz, P.G., Meltzer, C.C., Villemagne, V.L., Kinahan, P.E., Chander, S., Martinelli, M.A., and Townsend, D.W. (2000). Combined PET/CT imaging in oncology: Impact on patient management. *Clinical Positron Imaging* 3(6), 223-230.
- Korber, D.R., Lawrence, J.R., Woffaardt, G.M., and Caldwell, D.E. (1993). *Analysis of Spatial Variability within MOT<sup>+</sup> and MOT<sup>-</sup> Pseudomonas fluorescens Biofilms Using Representative Elements*, Biofouling 7, 339-358.
- Kuehn, M., Hausner, M., Bungartz, H.-J., Wagner, M., Wilderer, P.A., and Wuertz, S. (1998). Automated Confocal Laser Scanning Microscopy and Semiautomated Image Processing for Analysis of Biofilms. *Applied and Environmental Microbiology* 64, 4115-4127.
- Lawrence, J.R., Korber, D.R., Wolfaardt, G.M., and Caldwell, D.E. (1997). Analytical Imaging and Microscopy Techniques. In: Hurst, C.J., Knudsen, G.R., McInemey, M.J., Stetzenbach, L.D., and Walter, M.V. (Ed.), *Manual of Environmental Microbiology*, 29-51. ASM Press, Washington, DC.
- Lewandowski, Z., Webb, D., Hamilton, M., and Harkin, G. (1999). Quantifying Biofilm Structure. *Water Science and Technology* 39, 71-76.
- McGraw, T., Vemuri, B.C., Chen, Y., Rao, M., and Mareci, T. (2004). DT-MRI denoising and neuronal fiber tracking. *Medical Image Analysis* 8, 95-111.
- Mitchell, H.L. (1995). Applications of Digital Photogrammetry to Medical Investigations. *ISPRS Journal of Photogrammetry and Remote Sensing* 50(3), 27-36.
- Moslemy, P., Guiot, S.R., and Neufeld, R.J. (2002). Production of Size-Controlled Gellan Gum Microbeads Encapsulating Gasoline-Degrading Bacteria. *Enzyme and Microbial Technology* 30, 10-18.
- Neto, C.C.P., Roman, C., Johnson, M., Jagasia, M., Martin, W.H., and Delbeke, D. (2004). Positron emission tomography/ Computed tomography of a rare xanthogranulomatous process: Erdheim-Chester disease. *Molecular Imaging and Biology* 6, 1, pp. 63-67.
- Paling, S.M., Williams, E.D., Barber, R., Burton, E.J., Crum, W.R., Fox, N.C., and O'Brien, J.T. (2004). The application of serial MRI analysis techniques to the study of cerebral atrophy in late-onset dementia, *Medical Image Analysis* 8, 69-79.
- Park S.-W., Leeb, J.-H., Ehara, S., Park Y.-B., Sung S.O., Choi J.-A., and Joo Y.E. (2004). Single shot fast spin echo diffusion-weighted MR imaging of the spine: Is it useful in differentiating malignant metastatic tumor infiltration from benign fracture edema? *Journal of Clinical Imaging* 28, 102-108.



- Petrișor, A.I., Kawaguchi, T., and Decho, A.W. (2003). An introduction to bacterial geography. In: Țepelea I., Antal C. (Ed.), *Proceedings of the 27th Annual Congress of the American-Romanian Academy of Arts and Sciences*, vol. 1, 158-162. Polytechnic International Press, Montreal.
- Petrișor A.I., and Decho A.W. (2004). Using geographical information techniques to quantify the spatial structure of endolithic boring processes within sediment grains of marine stromatolites. *Journal of Microbiological Methods* 56(2), 173-180.
- Petrișor A.I., and Decho A.W. (2006). Analysis of the Orientation of Cyanobacteria in Bahamian Stromatolite Mats Using a Digital Image Analysis and GIS-Based Approach. *Studia Universitatis Babes-Bolyai: Biologia* 51(1), 71-81.
- Petrișor A.I., Decho A.W. (2007). A novel computer-assisted approach using GIS and digital image analysis to estimate differences in concentrations of heterogeneous dispersed particles in solutions. *Buletinul Institutului Politehnic din Iași - tomul Chimie și inginerie chimică* 3-4, 31-36.
- Petrișor A.I., Cuc A.I., and Decho A.W. (2004a). Reconstruction and Computation of Microscale Biovolumes Using Geographical Information Systems: Potential Difficulties. *Research in Microbiology* 155(6), 447-454.
- Petrișor A.I., Kawaguchi T., and Decho A.W. (2004b). Quantifying CaCO<sub>3</sub> Microprecipitates within Developing Surface Mats of Marine Stromatolites using GIS and Digital Image Analysis. *Geomicrobiology Journal* 21(8), 491-496.
- Reid, R.P., Visscher, P.T., Decho, A.W., Stolz, J., Bebout, B.M., MacIntyre, I.G., Paerl, H.W., Pinckney, J.L., Prufert-Bebout, L., Steppe, T.F., and Des Marais, D.J. (2000). The role of microbes in the accretion, lamination and early lithification of modern marine stromatolites. *Nature* 406, 989-992.
- Stoodley, P. Sauer, K., Davies, D.G., and Costerton, J.W. (2002). Biofilms as Complex Differentiated Communities. *Annual Review of Microbiology* 56, 187-209.
- Timofti, N. (2004). *Methods for Estimating the Thickness of the Peat Layer - Algorithm for a Nondestructive Method*. Unpublished Bachelor's thesis, University of Bucharest, Bucharest.
- University of South Carolina (2003). USC Remote Sensing, retrieved 11/25/2003 from <http://www.cla.sc.edu/geog/rsrab/>.
- Yazgan, C., Fitoz, S., Atasoy, C., Turkolmez, K., Yagci, C., and Akyar, S. (2004). Virtual cystoscopy in the evaluation of bladder tumors. *Journal of Clinical Imaging* 28, 138-142.